The influence of impact angle on the dynamic response of a Hybrid III headform and brain tissue deformation

Authors:
Anna Oeur, Department of Human Kinetics, University of Ottawa, 200 Lees A106, Ottawa, ON, K1S 5S9, CAN. Phone: 1-613-562-5800 ext. 7207. Email: aoeur016@uottawa.ca

T Blaine Hoshizaki, Department of Human Kinetics, University of Ottawa, 200 Lees A106, Ottawa, ON, K1S 5S9, CAN. Phone: 1-613-562-5851. Email: thoshiza@uottawa.ca

Michael D Gilchrist, School of Mechanical and Materials Engineering, University College Dublin, Dublin, Belfield 4, IRL. Phone: +353-1-2830534. Email: Michael.gilchrist@ucd.ie

Abstract

The objective of this study was to investigate the influence of impact angle on the dynamic response of a Hybrid III headform and brain tissue deformation by impacting the front and side of the headform with four angle conditions (0° at the impact site and 5°, 10° and 15° counter-clockwise rotations from 0°) as well as three additional angles of -5°, -10° and -15° (clockwise rotations from 0°) at the side location to examine the effect of direction. The acceleration-time curves were used as input into a finite element model of the brain where maximum principal strain was calculated. The results from this study show that impact angle has an asymmetrical influence on headform dynamic responses and strain. An increase in impact angle tends to result in a growth of headform linear and rotational acceleration and maximum principal strain for the front location as well as the negative angles (0 to -15°) at the side, however varying trends were observed for the positive angles (from 0° to 15°) at the side. When developing sophisticated impact protocols and undertaking head injury reconstruction research, it is important to be aware of impact angle.

Keywords: Head impact angle, Hybrid III headform, Finite element analysis,

Introduction

Head injury affects a large proportion of the population with over two million people affected annually [1]. The outcomes associated with head injury have been known to affect daily life at work or school [2, 3] with more fatal consequences resulting in death. Head injury can be caused by an impact resulting in motion of the head and brain, where energy from the impact is transferred to the brain causing injury [4, 5]. Past studies have established a link between head motion and the resulting brain injury [6, 7] where researchers have used engineering metrics such as head acceleration and brain tissue deformation metrics to quantify the severity of head impacts [8].

A head impact event can be described using parameters such as impact mass, velocity, compliance, location and angle. Past research, has found that each of these variables affect the results of a head impact. Impact mass and velocity have been shown to vary the magnitudes of acceleration and impact force experienced by the headform with higher masses and velocities increasing the risk for injury [9-11]. Factors affecting the compliance of the impact condition have also been shown to be important when studying a head injuring event. Some components of head impact compliance could be manipulated by changing the stiffness of the materials involved in the impact, for example the energy absorbing liners in helmets. These liners contribute to influencing the amount of impact energy transferred to the head and thus reducing the risk for injury [10, 12].

The results of a head impact have been shown to be sensitive to impact location. This has been found from experimental research using animals as well as from computational research employing finite element analysis, where the impact location changes the severity and duration of concussive symptoms in animals [6] and the magnitudes of brain tissue deformation in finite

element models of the human brain [13]. Thus far, impact mass, compliance and location has been found to effect head impact response however research examining impact angle as a variable is less clear.

One study combined both impact location and 45° angles in producing centric (through the center of gravity) and non-centric (not through centre of gravity) impacts to the headform and found that linear dominant head accelerations were mainly from centric impacts and rotationally dominant accelerations were created by non-centric impacts [14]. These types of impact conditions have been found to influence the magnitudes of headform acceleration and brain tissue deformation contributing to the risk of brain injury [14, 15]. When examining these studies in light of impact angle, the orientation of the hemispherical impactor striker (Figure 1) used in this research created interactions between the striker and the headform that made isolating the influence of angle difficult. For example, when the striker is set up for a non-centric impact, the center of the striker may be directed at one location but the side of the striker would come into contact with a different location on the headform first [14].

In a separate study, researchers examined the headform dynamic response as a consequence of varying impact angles from -15 to +15° [16]. The authors reported that impact angle influences headform dynamic response, in particularly the x-, y- and z- components [16]. This study was limited to only examining headform dynamic response as a result of modulating impact angle and the risk of brain injury employing finite element analysis has yet to be studied. As similar to the previous work by [14, 15], the surface of the striker is a major factor on isolating the effect of angle on headform dynamic response. The work presented by Walsh & Hoshizaki [16] used a flat modular elastomer programmer (MEP) striker which presents similar

issues with the sides of the striker coming into contact with the headform first when varying the impact angle.

As mentioned, research varying the inbound angle of an impactor often created conditions where a different site on the headform was impacted. Consequently, the objective of this present study was to isolate impact angle as a variable by impacting the same location on a headform at different incoming angles and to examine this influence on brain tissue deformation. Headform dynamic response was measured using linear and rotational accelerations and used as input into a finite element model of the brain to calculate magnitudes of maximum principal strain.

Methodology

Equipment

A pneumatic linear impactor system was used to deliver impacts to a headform. The linear impactor system was composed of a steel frame, piston, air tank and impactor arm (mass: 13.1 kg). The impactor arm was propelled forward using compressed air and was covered with a pointed striker that had a layer of modular elastomer programmer (MEP). The MEP layer was 25.0 ± 1 mm thick and was placed between a 25.0 ± 1 mm thick vinyl layer base and a vinyl rounded tip (Figure 2). This striker was different from the hemispherical striker used in past research [14, 15] because it had a much narrower cap that allowed the same location on the headform to be impacted at different angles. A sliding table located at the end of the impactor arm attached the headform to an adjustable and lockable base. This allowed the headform to be oriented and remain fixed in space during testing. This feature allowed the headform to be oriented in five degrees of freedom: anterior-posterior (x), lateral (y) and superior-inferior (z) translation as well as anterior-posterior (y) and longitudinal rotation (z) with positive x, y and z axes moving forwards, leftwards and upwards.

Figure 1. Hemispherical MEP impactor striker

A 50th percentile adult male Hybrid III head and neckform were used to collect the dynamic response of the head. The surrogates were composed of a combination of steel, aluminum, butyl rubber and vinyl where the headform weighed 4.54 ± 0.01 kg and the neckform weighed 1.54 ± 0.05 kg. The headform was equipped with 9 single-axis Endevco 7264C-2KTZ-2-300 accelerometers that were arranged in a 3-2-2-2 array to collect headform acceleration data [17].

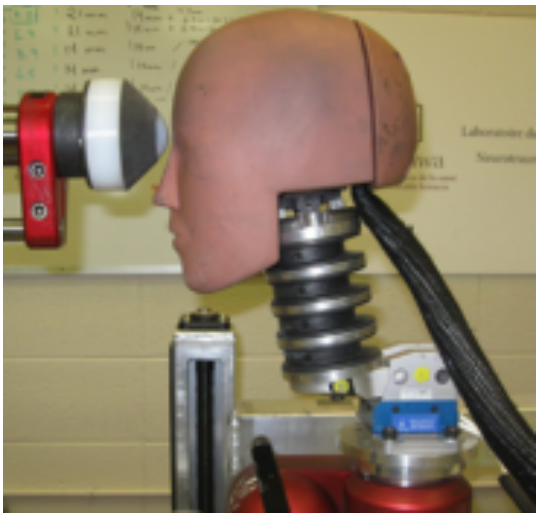

Figure 2 Hybrid III head and neckform with pointed MEP striker impactor (front condition)

Data Collection

Linear and rotational acceleration data was collected at a rate of 20 kHz when the headform acceleration exceeded a threshold level of 3 g. This data was recorded on a personal

computer using TDAS Pro Lab computer software (Diversified Technical Systems, Seal Beach, California). An electronic time gate was used to calculate impact velocity by measuring the time it took for a 0.02525 m flag to pass through a laser beam. This data was captured and analyzed using National Instruments VI-Logger (Austin Massachusetts, Texas) and Bioproc 2 (developed by D.G.E. Robertson, University of Ottawa).

Procedure

The headform was impacted at the front and side location using 4 angle conditions: a 0° condition (perpendicular to the impact location) and a 5, 10 and 15° condition (counter-clockwise rotation of the headform in the transverse plane from the 0° condition) (Figure 3**Error! Reference source not found.**). Three additional impact angle conditions were used at the side location, -5, -10 and -15° clockwise rotations of the headform to evaluate the effect of direction. Impact site accuracy was ensured prior to each impact condition through the use of a laser that was mounted to the center of the impactor arm and that matched marked locations on the headform (front and side 0° conditions). Care was taken to ensure that the first point of contact between the apex of the striker and the headform was at the same location for all angles. The maximum angle of 15° was limited by the pointed MEP striker used because each condition had to impact the same site on the headform throughout the different angles. Therefore, larger angles greater than 15° created conditions where the side of the striker came into contact with the headform first. The headform was impacted three times per condition at a velocity of 5.5 m/s for a total of 33 impacts.

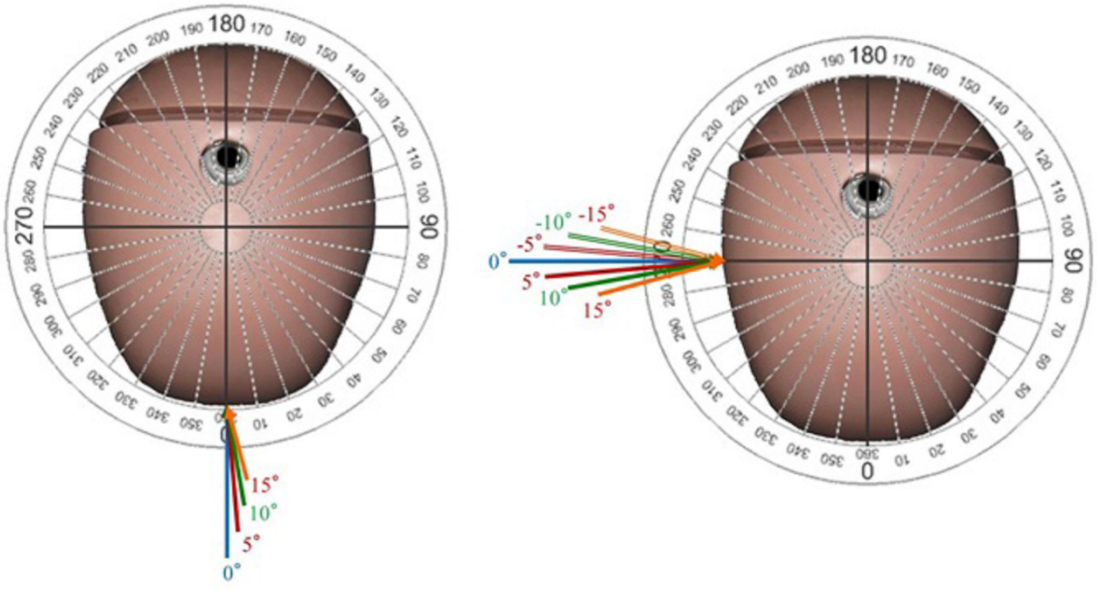

Figure 3. Front and side impact conditions. Left image illustrates the 0°, 5°, 10°, and 15° angles for the front location, right image illustrates the impact angles at the side location for both positive and negative angles.

Finite element model

The finite element model used in this study was the University College Dublin Brain Trauma Model (UCDBTM). Discretization of the model was done using computed tomography (CT) and magnetic resonance imaging (MRI) scans of a male human cadaver [18, 19]. The model is composed of approximately 26 000 elements constituting the scalp, skull, pia, falx, tentorium, white and grey matter as well as cerebrospinal fluid (CSF) [19]. To approximate the slip layer of the CSF, elements representing this component were solid elements with a lower shear moduli to allow shear motion between the skull and brain [19]. The characteristics of the different tissues of the brain were taken from the literature and are listed in Table 1**Error! Reference source not found.** and Table 3 [18, 19]. The linear viscoelastic behavior of the brain tissue is represented with the following shear modulus equation:

$$G(t) = G_\infty + (G_0 - G_\infty)e^{-\beta t}$$

where G_∞ and G_0 represent the long- and short-term moduli and β represents the decay factor of the material [18, 19]. A unique G_∞ and G_0 constant for each tissue is representative of the time dependent response of that particular tissue to shear loading. Validation of the model was conducted through comparisons with experimental cadaver head impact data measuring intracranial pressures and accelerations as well as relative brain and skull surface motion results [18-22].

The three-dimensional linear and rotational acceleration-time curves from the bare headform impacts were used as input into the finite element model to estimate brain tissue deformation. The brain tissue deformation metric used in this study was maximum principal strain (MPS), which is a measure that has been used in the past [23, 24] to quantify brain deformation associated with head impacts.

Table 1. University College Dublin Brain Trauma Model Properties

Material	Young's Modulus, MPa	Poisson's Ratio	Density, kg/m³
Scalp	16.7	0.42	1000
Cortical Bone	15 000	0.22	2000
Trabecular Bone	1000	0.24	1300
Dura	31.5	0.45	1130
Pia	11.5	0.45	1130
Falx	31.5	0.45	1140
Tentorium	31.5	0.45	1140
CSF	-	0.5	1000
White Matter	Hyperelastic	0.499997	1060
Grey Matter	Hyperelastic	0.499998	1060

Table 3. Tissue characteristics for UCDBTM

	Shear Modulus, kPa		Decay Constant, s^{-1}	Bulk Modulus, GPa
	G_0	G_∞		
Grey Matter	10	2.0	80	2.19
White Matter	12.5	2.5	80	2.19
Brain Stem	22.5	4.5	80	2.19
Cerebellum	10	2.0	80	2.19

Statistical Analyses

A total of six one-way ANOVAs were used to compare the effect of impact angle on each of the dependent variables (peak linear and rotational acceleration and maximum principal strain) for the front and side locations. When a significant main effect for impact angle was detected, post hoc analyses was performed using the Tukey method. The alpha level was set to $p<0.05$ in all tests and was conducted using SPSS 16.0 for Windows (SPSS Inc. Chicago, IL, USA).

Results

Table 4**Error! Reference source not found.** lists the results for mean peak resultant linear and rotational accelerations as well as maximum principal strain for all impact angle conditions. For peak resultant linear acceleration, a main effect was only detected for the side location [$F(6, 14) = 7.001$, $p = 0.001$] where the -15° condition produced a significantly higher response than the -5° condition ($p=0.05$). A different relationship was found for rotational acceleration. A main effect of angle was detected at the front location [$F(3, 8) = 124.50$, $p < 0.001$] where the 15° angle produced significantly higher rotational accelerations than the 0°, 5°, and 10° angles ($p<0.05$). The 10° condition also produced significantly higher rotational accelerations than the 0° and 5° conditions ($P<0.05$). Similarly, a main effect of angle was found for the side location [$F(6, 14) = 5.14$, $p=0.006$], where the -15° condition produced higher rotational accelerations than the 0 and -5° conditions ($p=0.039$ and $p=0.002$, respectively). A main effect of angle was detected for maximum principal strain [$F(3, 8) = 12.13$, $p=0.002$) at the front location with the 15° condition producing higher MPS values than the 0 and 5° condition ($p<0.05$). At the side location, a main effect of angle was detected [$F(6, 14) = 0.004$, $p<0.001$] where the 15°

condition produced higher MPS values than the 10° condition ($p=0.024$). For the negative impact angles, both the -10 and -15° conditions produced significantly higher MPS values than the 0 and -5° conditions ($p<0.05$).

Table 4. Peak resultant accelerations and maximum principal strain for each impact condition

Location	Angle, °	Peak Linear Acceleration, g	Peak Angular Acceleration, rad/s²	Maximum Principal Strain
Front	0	165.6 (0.9)	8083 (187)	0.515 (0.03)
	5	162.2 (3.3)	8282 (102)	0.496 (0.04)
	10	165.6 (5.6)	8778 (128)	0.558 (0.01)
	15	169.8 (1.6)	9939 (70)	0.610 (0.01)
Side	-15	174.5 (4.0)	11964 (346)	0.634 (0.02)
	-10	171.7 (2.1)	11145 (106)	0.602 (0.01)
	-5	164.5 (3.0)	10642 (603)	0.561 (0.02)
	0	164.7 (7.1)	11067 (244)	0.557 (0.02)
	5	162.3 (2.6)	10934 (153)	0.548 (0.01)
	10	161.4 (0.7)	11034 (136)	0.527 (0.01)
	15	159.8 (1.5)	11121 (275)	0.568 (0.01)

Discussion

The values of linear acceleration for a direct head impact in this study (160-170 g) were found to be lower than those reported for experimental cadaver test number 37 (200 g) by Nahum, Smith and Ward [20]. The difference in peak values could be attributed to the variability in impact conditions specified for each study. For example the impactor mass and velocity used in each experiment was not the same. The test conditions for Nahum et al. [20] employed an impactor mass of 5.59 kg at a velocity of 9.94 m/s as compared to this study with an impactor mass of 13.1 kg and a velocity of 5.5 m/s. Secondly, the impactors used in each study may have not been the same. The characteristics of the impactor, such as compliance have been found to

have an effect on the headform response [25]. A smaller impactor striker, such as the one used in this study produced approximately half the values of headform dynamic response when compared to a much larger hemispherical striker (Figure 1) [25]. The smaller striker was comprised of much less MEP material causing it to be more compliant leading to less transfer of energy to the headform at impact [25].

When examining the results as reported in Table 3 for peak resultant linear and rotational accelerations, the magnitude of differences across all conditions of angle is small and that statistical significance found in this study is a reflection of the reliability of the testing equipment between trials.

To better illustrate the influence of angle on headform dynamic response, peak x-, y-, z-axes and resultant linear and rotational accelerations were plotted for each angle condition at the front and side locations (Figure 5 and Figure 6, respectively). For the front location, peak resultant linear accelerations (black line) remains relatively level indicating that the magnitude of differences as a result of varying angle may be inconsequential as there is little difference between peak resultant values . A similar trend can be observed for the side location, although the line tends to slightly increase moving from 15° to -15°, it is important to keep in mind the difference between responses from these conditions is 15 g.

When examining peak resultant rotational acceleration (black line) in Figures 4 and 5, an increase in impact angle results in a growth in rotational response. This trend is clear for the front location however at the side location this growth is dependent on the direction of the applied vector (as seen for negative angles). This increase in rotational response is expected as the impact vector becomes oriented away from the centre of gravity of the headform. The trends observed for headform dynamic response is affected by interaction between the surface of

impactor striker, headform geometry and headform skin where the interaction between these factors may create a direction dependent response at the side which is likely due to the geometry of the headform for impact vectors oriented in a counter-clockwise fashion (negative angles).

The Hybrid III headform does not have a uniform mass distribution, which would affect the moment of the inertia of the headform. The moments of inertia of a Hybrid III headform are $1.590 \cdot 10^{-2}\,kg \cdot m^2$ in the x-axis, $2.400 \cdot 10^{-2}\,kg \cdot m^2$ in the y-axis and $2.200 \cdot 10^{-2}\,kg \cdot m^2$ in the z-axes, with positive axes oriented frontwards, leftwards and upwards respectively [26]. A lower moment of inertia in the x-axis would contribute to the larger magnitudes of rotational acceleration seen for side impacts relative to frontal impacts.

Characteristics of the neckform could have contributed to affecting the dynamic response as well. The Hybrid III neckform has slits on the anterior portion of the neck which allow for different neck responses in flexion than extension [27]. Under quasi-static bending tests, frontal loading (extension) was found to be more compliant than lateral loading (side bending, and rear loading (neck flexion) [28]. These anisotropic characteristics of the neckform have been found to contribute to influencing the magnitudes of headform acceleration [28].

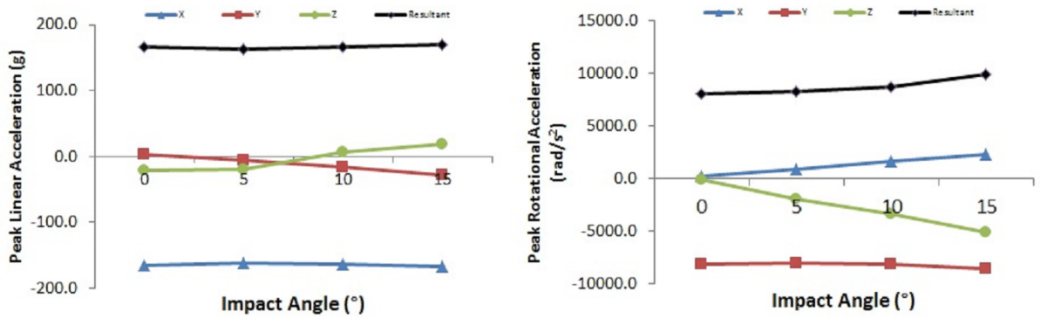

Figure 5. X, Y, Z, and resultant peak linear (left) and rotational (right) accelerations for each impact angle at the front location

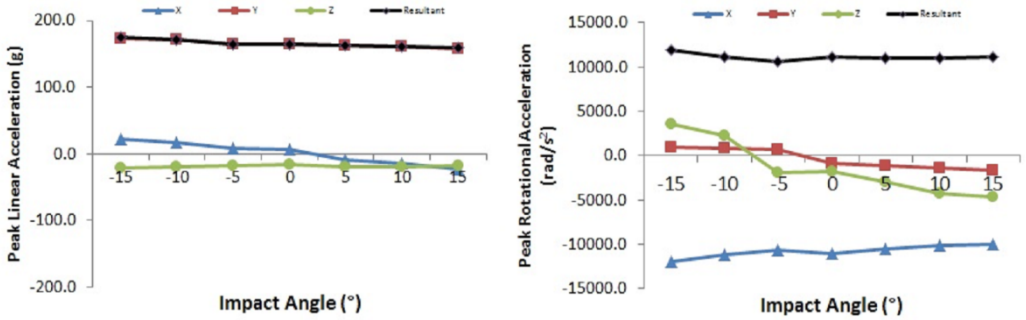

Figure 6. X, Y, Z, and resultant peak linear (left) and rotational (right) accelerations for each impact angle at the side location

The trends for peak maximum principal strain (MPS) are similar to those observed for linear and rotational acceleration where an increase in impact angle caused a growth in strain values for the front location and for the negative angles at the side. For the positive angles at the side, the effect of angle was more varied. Finite element analysis allows for the evaluation of brain tissue deformation using six vectors (x, y, z axes) of headform linear and rotation accelerations from an impact [18, 29]. This similarity in trends reported for strain and dynamic response was expected since the strain values were derived from the acceleration-time histories recorded using the Hybrid III headform.

This can be illustrated by examining the component x, y and z axis accelerations (Figures 4 and 5), the magnitude of one axis of acceleration is closely reflected by the resultant (black line), meanwhile the other two axes, although much lower in magnitude tend to fluctuate. Since MPS takes into consideration all axes of acceleration, these fluctuations contribute to the overall trends observed for strain. These findings are in accordance with those reported by Walsh & Hoshizaki [16], where a change in inbound angle of a flat anvil altered the component accelerations responses for bare headform impacts.

The large values of strain observed in this study are likely a reflection of the characteristics of the acceleration-time curves for each condition of angle. Characteristics such as curve shape,

magnitude, and duration of the acceleration pulse has been shown to effect brain tissue deformation values obtained from finite element analysis [29, 30]. Exemplar acceleration-time histories for the front location are shown in Figures 6 and 7. In this study, the duration of the initial resultant acceleration pulse is within 7ms for both linear and rotational acceleration, which was similar to test number 37 by Nahum et al. [20]. Similar to the peak resultant values, the fluctuations in acceleration components are also observed over time. As mentioned above, these fluctuations in component axes of acceleration affect the calculated strain results derived from finite element analysis.

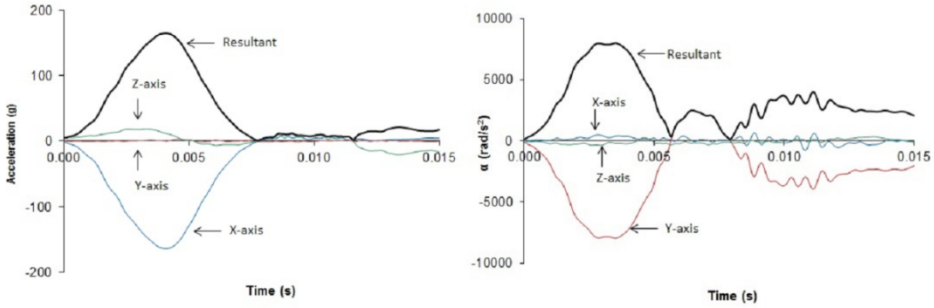

Figure 7. Linear (left) and rotational (right) acceleration-time histories for the 0° impact angle at the front location

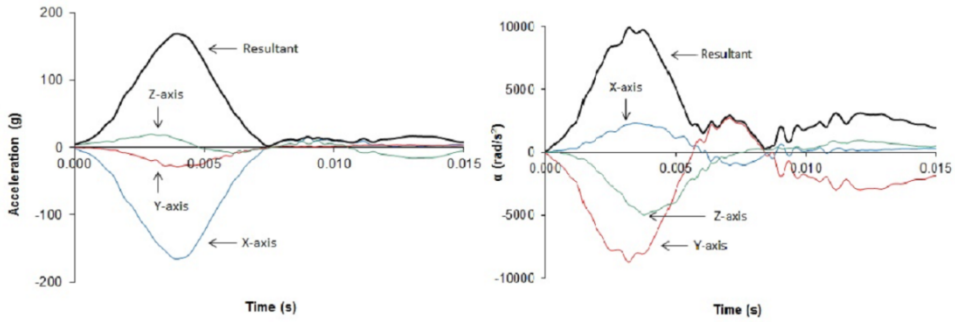

Figure 8. Linear (left) and rotational (right) acceleration-time histories for the 15° impact angle at the front location

The results from this study show that impact angle has an asymmetrical influence on headform dynamic responses and brain tissue deformations. An increase in impact angle tends to result in a growth of headform linear and rotational acceleration and maximum principal strain

for the front location as well as the negative angles (0 to -15°) at the side, however the results for the positive angles (from 0° to 15°) at the side produced much more variable responses. Therefore, when developing sophisticated centric and non-centric impact protocols and undertaking head injury reconstruction research, it is important to be aware of impact angle as a variable influencing the impact condition.

Limitations

The Hybrid III head and neckform are limitations of this study because they are used as human surrogates to head impact. These surrogates are composed of a combination of metal and rubber and may not be representative of a living human's response to impact. Similarly, the finite element model used in this study is also a limitation because it estimates human brain tissue deformations based on a number of assumptions regarding the behavior of brain tissue properties and its validation. The finite element model was validated against cadaver head impact research and may not provide an accurate estimation of living human brain tissue deformation to impact, which would make it difficult for use in predicting brain injury. The pointed impactor striker was also a limitation of this study because the geometry of the striker limited the maximum variation of impact angle to 15°. However, impacts directed beyond 15° using this striker created conditions where the side of the striker impacted the headform which did not allow for impact angle as a variable to be isolated and studied. To obtain more impact angle variations, a more acutely pointed striker would be needed; however the more narrow the tip of the impactor cap becomes, the mechanism of injury becomes more of a penetration type of injury.

Secondly, scaling the finite element model to the dimensions of the Hybrid III headform was not completed in this study, which is also a limitation of the work presented. The dimensions

of the brain finite element model have been known to affect the magnitudes of stress [31] and may have similar consequences for strain. However, the results presented herein would continue to reflect the impact angle phenomena since the head and brain dimensions were kept constant for all conditions of angle.

Delimitations

This study was delimited to the 50th percentile adult male Hybrid III headform. Although female versions of the headform have been developed, the male headform was readily available in laboratory for use in this study. While different headforms would produce characteristic responses to impact, the objective of this study was to investigate impact angle on the response of a headform, therefore it is assumed that these relationships would be similar, despite the specific headform used. This study was also delimited to the front and side impact location as well as the 0, 5, 10 and 15° impact angles. The locations were chosen because they represent different geometries associated with the head and the angles were chosen because these angles permitted the same location on the headform to be impacted at different angles given the geometry of the impactor striker.

References

[1] Langlois, J.A., Rutland-Brown, W. and Wald, M.M., "The epidemiology and impact of traumatic brain injury," *J Head Trauma Rehabil.*, Vol. 21, 2006, pp. 375-378.

[2] McCrea, M., Guskiewicz, K.M, Marshall, S.W., Barr, W., Randolph, C., Cantu, R.C., Onate, J.A., Yang, J. and Kelly, J.P., "Acute Effects and Recovery Time Following Concussion in Collegiate Football Players: The NCAA Concussion Study," *JAMA*, Vol. 290, 2003, pp. 2556-2563.

[3] van Donkelaar, P., Langan, J., Rodriguez, E., Drew, A., Halterman, C., Osternig, L.R. and Chou, L-S., "Attentional Deficits in Concussion," *Brain Injury*, Vol 19, 2005, pp. 1031-1039.

[4] Groat, R.A., Windle, W.F. and Magoun, H.W., "Functional and Structural Changes in the Monkey's Brain during and After Concussion," *J Neurosurgery*, Vol. 2, 1945, pp. 26-35.

[5] Meaney, D.F. and Smith, D.H., "Biomechanics of Concussion," *Clin Sports Med*, Vol. 30, 2011, pp. 19-31.

[6] Gennarelli, T.A., Thibault, L.E., Adams, J.H., Grahams, D.I., Thompson, C.J. and Marcincin, R.P., "Diffuse Axonal Injury and Traumatic Coma in the Primate," *Ann Neurol*, Vol. 12, 1982, pp. 564-574.

[7] Unterharnscheidt, F.J., "Translational versus Rotational Acceleration: Animal Experiments with Measured Input," *Scand J Rehabil Med*, Vol. 4, 1972, pp. 24-26.

[8] Zhang, L., Yang, K.H. and King, A.I, "A Proposed Injury Threshold for Mild Traumatic Brain Injury," *J Biomech Eng*, Vol. 126, 2004, pp. 226-236.

[9] Gimbel, G.M. and Hoshizaki, T.B, "Compressive Properties of Helmet Materials Subjected to Dynamic Helmet Loading of Various Energies," *Eur J Sport Sci*, Vol. 8, 2008, pp. 341-349.

[10] Hoshizaki, B., Vassilyadi, M., Post, A. and Oeur, A, "Performance Analysis of Winter Activity Head Gear for Young Children," *J Neurosurg Pediatr*, Vol. 9, 2012, pp. 133-138.

[11] Karton, C. (2012). The effect of inbound mass on the dynamic response of the Hybrid III headform and brain tissue deformation. MSc. Thesis. University of Ottawa, Ottawa, Canada.

[12] Spyrou, E., Pearsall, D.J. and Hoshizaki, T.B, "Effect of Local Shell Geometry and Material Properties on Impact Attenuation of Ice Hockey Helmets," *Sports Engineering*, Vol. 3, 2000, pp. 25-35.

[13] Zhang, L., Yang, K.H. and King, A.I, "Comparison of Brain Responses between Frontal and Lateral Impacts by Finite Element Modeling," *J Neurotrauma*, Vol. 18, 2001, pp. 21-30.

[14] Walsh, E.S., Rousseau, P. and Hoshizaki, T.B., "The Influence of Impact Location and Angle on the Dynamic Response of a Hybrid III Headform," *Sports Engineering*, Vol. 13, 2011, pp. 135-143.

[15] Post, A., Oeur, A., Hoshizaki, T.B and Gilchrist, M.D., "Examination of the Relationship between Peak Linear and Angular Accelerations to Brain Deformation Metrics in Hockey Helmet Impacts," *Comput Methods Biomech Biomed Engin*, Vol. 16(5), 2011, pp.511-519.

[16] Walsh, E.S., Hoshizaki, T.B. (July, 2010). Sensitivity analysis of a Hybrid III head- and neckform to impact angle variations. *8th Conference of the International Sports Engineering Association*, Vienna, Austria. 12-16 July, International Sports Engineering Association, Centre for Sports Engineering Research, Sheffield, U.K.

[17] Padgaonkar, A.J., Kreiger, K.W. and King, A.I., "Measurement of Angular Accelerations of a Rigid Body using Linear Accelerations," *J App Mech*, Vol. 42, 1975, pp. 552-556.

[18] Horgan, T. J., & Gilchrist, M. D. (2003). The creation of three-dimensional finite element models for simulating head impact biomechanics. *International Journal of Crashworthiness, 8*(4), 353-366
[19] Horgan, T.J. and Gilchrist, M.D., "Influence of FE model Variability in Predicting Brain Motion and Intracranial Pressure Changes in Head Impact Simulations," *Int. J. Crash*, Vol. 9, 2004, pp. 401-418.
[20] Nahum, A.M., Smith, R. and Ward, C.C. "Intracranial pressure dynamics during head impact". , *SAE* Technical paper 770922, 1977, SAE International, Warrendale, USA.
[21] Hardy, W.N., Foster, C.D., Mason, M.J., Yang, K.H., King, A.I., Tashman, S. (2001). Investigation of head injury mechanisms using neutral density technology and high-speed biplanar x-ray. *Stapp Car Crash J*, 45. 337-368.
[22] Trosseille, X., Tarriere, C., Lavaste, F., Guillon, F., & Domont, A. "Development of a FEM of the human head according to a specific test protocol", *SAE* Technical paper 922527, 1992, SAE International Warrendale, USA.
[23] Kleiven, S. "Predictors for Traumatic Brain Injuries Evaluated through Accident Reconstructions. *Stapp Car Crash J*, Vol. 51, 2007, pp. 81-114.
[24] Willinger, R., Baumgartner, D. (2003). Human head tolerance limits to specific injury mechanisms. *Int. J. Crash,* 8(6), 605-617.
[25] Dawson, L., Oeur, A., Rousseau, P., Hoshizaki, T.B. (2012). The influence of striker cap size on the dynamic response of a Hybrid III headform. Journal of ASTM International. Submitted 11/19/2012.
[26] Willinger, R., Baumgartner, D., Chinn, R., Schuller, E. (2001). New dummy head prototype: development, validation and injury criteria. *Int. J. Crash*, 6(3), 281-294.
[27] Ashrafiuon, H., Colbert, R., Obergefell, L. and Kaleps, I., "Modeling of a Deformable Manikin Neck for Multibody Dynamic Simulation. *Mat. Comp. Mod*. Vol. 24, 1996, pp. 45-56
[28] Foreman, S. (2010). The dynamic impact response of a Hybrid III head- and neckform under four neck orientations and three impact locations. MSc. Thesis. University of Ottawa, Ottawa, Canada.
[29] Post, A., Hoshizaki, T.B., Gilchrist, M.D. (2012). Finite element analysis of the effect of loading curve shape on injury predictors. *Journal of Biomechanics, 45*(1), 679-683
[30] Yoganandan, N., Li, J., Zhang, J., Pintar, F.A., Gennarelli, T.A. (2008). Influence of angular acceleration-deceleration pulse shapes on regional brain strains. *Journal of Biomechanics, 41*(10), 2253-2262
[31] Kleiven, S. & von Holst, H. (2002). Consequences of head size following trauma to the human head. *Journal of Biomechanics, 35*(2), 153-160.